

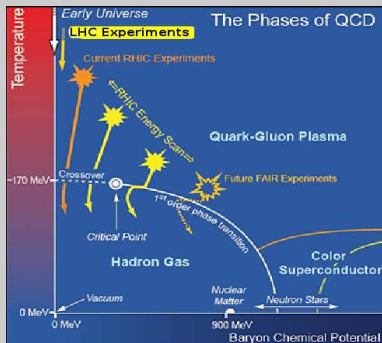
# QCD Thermodynamics up to three loop at finite $T$ and $\mu$

**NAJMUL HAQUE**

Theory Division,  
Saha institute of Nuclear Physics  
Kolkata, India

# QCD Phase Diagram & EoS

- At High temperature and/or density Quarks and Gluons become deconfined and produce QGP.
- In ongoing RHIC experiments and also future FAIR experiments the chemical potential of deconfined Nuclear matter is finite.
- Determination of EoS of hot and dense Nuclear matter is essential to QGP phenomenology.



# Thermodynamics using Lattice QCD

- The currently most reliable method for determining the equation of state at finite temperature is lattice QCD.
- Due to the sign problem, lattice QCD can not compute EoS at finite baryon chemical potential straightforwardly.
- It can compute thermodynamic functions at small chemical potential by making a Taylor expansion of the partition function around  $\mu = 0$  and extrapolating the result as

$$P(T, \mu) = P(T, \mu = 0) + \frac{\mu^2}{2} \left. \frac{\partial^2 P}{\partial \mu^2} \right|_{\mu=0} + \frac{\mu^4}{4!} \left. \frac{\partial^4 P}{\partial \mu^4} \right|_{\mu=0} + \dots$$

- The extrapolations can only be trusted at small chemical potential, it would be nice to have an alternative framework for calculating QCD thermodynamical quantities at finite  $T$  and  $\mu$ .

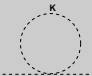
# Thermodynamics using perturbation theory

- At sufficiently high temperature, the value of the strong coupling constant is small  $\Rightarrow$  It works well at high  $T$ .
- Unfortunately, it turns out that a strict expansion in the coupling constant does not converge at the temperature those are relevant for heavy-ion collision experiments.
- The source of the poor convergence comes from contributions from soft momenta,  $p \sim gT$ .
- One needs a way of reorganizing the perturbative series which treats the soft sector more carefully.

# Hard Thermal Loop perturbation theory

- Hard Thermal Loop (HTL) perturbation theory is a gauge invariant reorganization of usual perturbation at finite temperature and finite chemical potential and higher order diagrams contribute to lower order.
- In HTL approximation we define *Two Scales of Momentum*
  - 1 Hard momentum:  $p_0, p \sim T$ .
  - 2 Soft momentum:  $p_0, p \sim gT$ .
- In HTL approximation we are interested in high temperature limits, so one can take **Loop Momentum  $\gg$  External Momentum**

Scalar case:

$$\Pi_1 = \text{Diagram} = g^2 T^2.$$


$$\text{Effective propagator } D^* = \frac{1}{P^2 - \Pi_1}$$

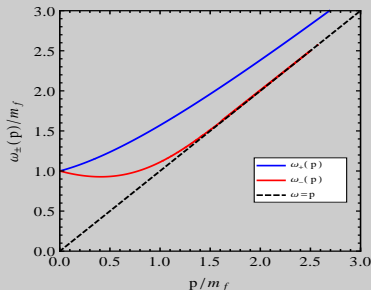
# HTL in gauge theory: Quark Propagator

Quark propagator:

$$iS^*(P) = \frac{1}{2} \left[ \frac{\gamma^0 - \vec{\gamma} \cdot \hat{p}}{D_+(P)} + \frac{\gamma^0 + \vec{\gamma} \cdot \hat{p}}{D_-(P)} \right].$$

$$D_{\pm}(p_0, p) = -p_0 \pm p + \frac{m_f^2}{p} \left[ \pm 1 + \frac{1}{2} \left( 1 \mp \frac{p_0}{p} \right) \ln \frac{p_0 + p}{p_0 - p} \right]$$

Dispersion relation:  $D_{\pm}(p_0, p) = 0$



- Total Lagrangian density:

$$\mathcal{L} = (\mathcal{L}_{\text{QCD}} + \mathcal{L}_{\text{HTL}})|_{g \rightarrow \sqrt{\delta}g} + \Delta\mathcal{L}_{\text{HTL}},$$

$$\mathcal{L}_{\text{HTL}} = (1 - \delta)im_q^2 \bar{\psi} \gamma^\mu \left\langle \frac{Y_\mu}{Y \cdot D} \right\rangle_{\hat{y}} \psi$$

$$- \frac{1}{2}(1 - \delta)m_D^2 \text{Tr} \left( F_{\mu\alpha} \left\langle \frac{Y^\alpha Y_\beta}{(Y \cdot D)^2} \right\rangle_{\hat{y}} F^{\mu\beta} \right),$$

- The HTLpt Lagrangian reduces to the QCD Lagrangian if we set  $\delta = 1$ .
- Physical observables are calculated in HTLpt by expanding in powers of  $\delta$ , truncating at some specified order, and then setting  $\delta = 1$ .
- $m_D$  and  $m_q$  are two parameters will be treated as Debye mass and thermal quark mass respectively.

# One loop HTL thermodynamics

The Feynman diagrams that will contribute to the thermodynamic potential in one loop:

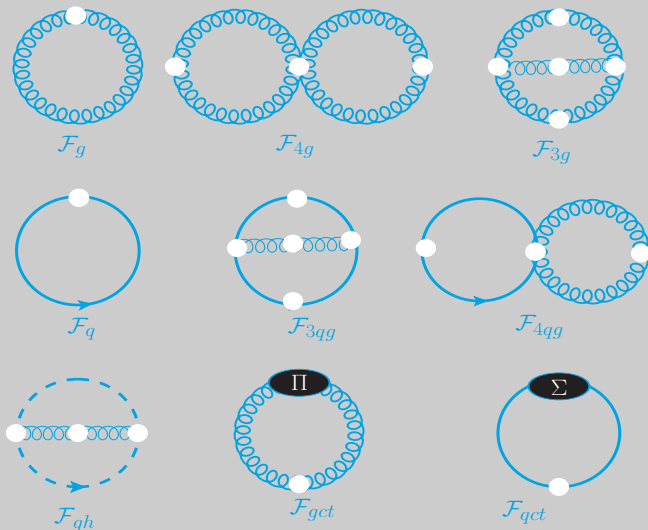


$$\begin{aligned}
 \mathcal{P}(T, \mu) = & 2N_f N_c T \int \frac{d^3k}{(2\pi)^3} \left[ \ln \left( 1 + e^{-\beta(\omega_+ - \mu)} \right) + \ln \left( \frac{1 + e^{-\beta(\omega_- - \mu)}}{1 + e^{-\beta(k - \mu)}} \right) \right. \\
 & + \ln \left( 1 + e^{-\beta(\omega_+ + \mu)} \right) + \ln \left( \frac{1 + e^{-\beta(\omega_- + \mu)}}{1 + e^{-\beta(k + \mu)}} \right) + \beta\omega_+ + \beta(\omega_- - k) \\
 & \left. + \int_{-k}^k d\omega \left( \frac{2m_q^2}{\omega^2 - k^2} \right) \beta_+(\omega, k) \left[ \ln \left( 1 + e^{-\beta(\omega - \mu)} \right) + \ln \left( 1 + e^{-\beta(\omega + \mu)} \right) + \beta\omega \right] \right] \\
 & + \text{Gluonic contribution}
 \end{aligned}$$

$$\rho = \frac{\partial \mathcal{P}}{\partial \mu}; \quad S = \frac{\partial \mathcal{P}}{\partial T}; \quad \chi = \frac{\partial^2 \mathcal{P}}{\partial \mu^2}$$

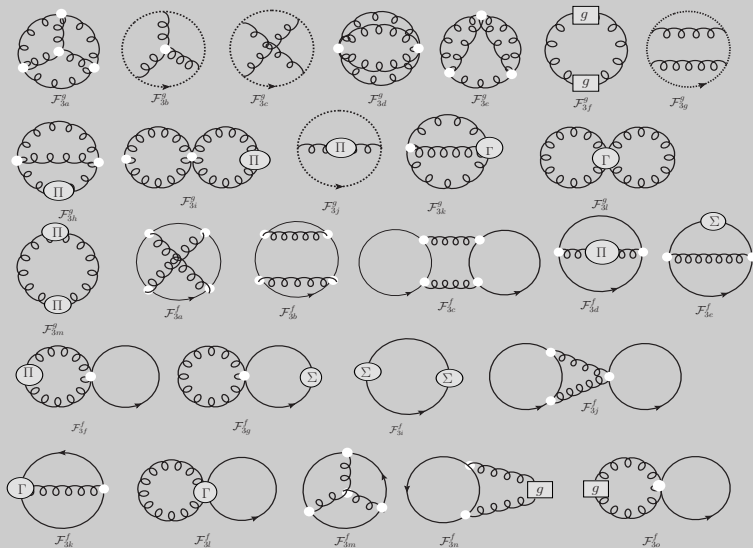


## Two loop HTL thermodynamics



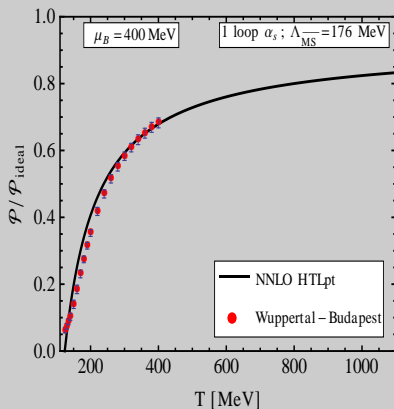
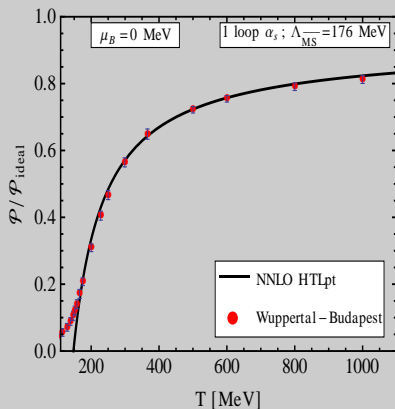
$$\begin{aligned}
\mathcal{P}_{\text{NLO}}(T, \mu) = & \\
d_A \frac{\pi^2 T^4}{45} & \left\{ 1 + \frac{7}{4} \frac{d_F}{d_A} \left( 1 + \frac{120}{7} \hat{\mu}^2 + \frac{240}{7} \hat{\mu}^4 \right) - 15 \hat{m}_D^3 - \frac{45}{4} \left( \log \frac{\hat{\Lambda}}{2} - \frac{7}{2} + \gamma + \frac{\pi^2}{3} \right) \hat{m}_D^4 \right. \\
& + 60 \frac{d_F}{d_A} (\pi^2 - 6) \hat{m}_q^4 + \frac{\alpha_s}{\pi} \left[ 15 (c_A + s_F (1 + 12 \hat{\mu}^2)) \hat{m}_D - \frac{5}{4} \left( c_A + \frac{5}{2} s_F \left( 1 + \frac{72}{5} \hat{\mu}^2 + \frac{144}{5} \hat{\mu}^4 \right) \right) \right. \\
& - \frac{55}{4} \left\{ c_A \left( \log \frac{\hat{\Lambda}}{2} - \frac{36}{11} \log \hat{m}_D - 2.001 \right) - \frac{4}{11} s_F \left[ \left( \log \frac{\hat{\Lambda}}{2} - 2.337 \right) \right. \right. \\
& + (24 - 18\zeta(3)) \left( \log \frac{\hat{\Lambda}}{2} - 15.662 \right) \hat{\mu}^2 + 120 (\zeta(5) - \zeta(3)) \left( \log \frac{\hat{\Lambda}}{2} - 1.5264 \right) \hat{\mu}^4 \left. \left. \right] \right\} \hat{m}_D^2 \\
& - 45 s_F \left\{ \log \frac{\hat{\Lambda}}{2} + 2.198 - 44.953 \hat{\mu}^2 - \left( 288 \ln \frac{\hat{\Lambda}}{2} + 19.836 \right) \hat{\mu}^4 \right\} \hat{m}_q^2 \\
& + \frac{165}{2} \left\{ c_A \left( \log \frac{\hat{\Lambda}}{2} + \frac{5}{22} + \gamma \right) - \frac{4}{11} s_F \left( \log \frac{\hat{\Lambda}}{2} - \frac{1}{2} + \gamma + 2 \ln 2 - 7\zeta(3) \hat{\mu}^2 + 31\zeta(5) \hat{\mu}^4 \right) \right\} \\
& + 15 s_F \left( 2 \frac{\zeta'(-1)}{\zeta(-1)} + 2 \ln \hat{m}_D \right) \left[ (24 - 18\zeta(3)) \hat{\mu}^2 + 120 (\zeta(5) - \zeta(3)) \hat{\mu}^4 \right] \hat{m}_D^3 + 180 s_F \hat{m}_D \hat{m}_q^2 \left. \right\}
\end{aligned}$$

# Three loop HTL thermodynamics



$$\begin{aligned}
\mathcal{P}_{\text{NNLO}} = & \frac{d_A \pi^2 T^4}{45} \left[ 1 + \frac{7}{4} \frac{d_F}{d_A} \left( 1 + \frac{120}{7} \hat{\mu}^2 + \frac{240}{7} \hat{\mu}^4 \right) - \frac{15}{4} \hat{m}_D^3 - \frac{s_F \alpha_s}{\pi} \left[ \frac{5}{8} \left( 5 + 72 \hat{\mu}^2 + 144 \hat{\mu}^4 \right) \right. \right. \\
& + 90 \hat{m}_q^2 \hat{m}_D - \frac{15}{2} \left( 1 + 12 \hat{\mu}^2 \right) \hat{m}_D - \frac{15}{2} \left( 2 \ln \frac{\hat{\Lambda}}{2} - 1 - \mathfrak{N}(z) \right) \hat{m}_D^3 \left. \right] + s_{2F} \left( \frac{\alpha_s}{\pi} \right)^2 \left[ - \frac{45}{2} \hat{m}_D \left( 1 + 12 \hat{\mu}^2 \right) \right. \\
& + \frac{15}{64} \left\{ 35 - 32 \left( 1 - 12 \hat{\mu}^2 \right) \frac{\zeta'(-1)}{\zeta(-1)} + 472 \hat{\mu}^2 + 1328 \hat{\mu}^4 + 64 \left( 6(1 + 8 \hat{\mu}^2) \mathfrak{N}(1, z) + 3i \hat{\mu} (1 + 4 \hat{\mu}^2) \mathfrak{N}(0, z) \right) \right. \\
& \left. \left. - 36i \hat{\mu} \mathfrak{N}(2, z) \right) \right] + \left( \frac{s_F \alpha_s}{\pi} \right)^2 \left[ \frac{5}{4 \hat{m}_D} \left( 1 + 12 \hat{\mu}^2 \right)^2 + 30 \left( 1 + 12 \hat{\mu}^2 \right) \frac{\hat{m}_q^2}{\hat{m}_D} + \frac{25}{12} \left\{ \frac{1}{20} \left( 1 + 168 \hat{\mu}^2 + 2064 \hat{\mu}^4 \right) \right. \right. \\
& + \left( 1 + \frac{72}{5} \hat{\mu}^2 + \frac{144}{5} \hat{\mu}^4 \right) \ln \frac{\hat{\Lambda}}{2} + \frac{3 \gamma_E}{5} \left( 1 + 12 \hat{\mu}^2 \right)^2 - \frac{8}{5} \left( 1 + 12 \hat{\mu}^2 \right) \frac{\zeta'(-1)}{\zeta(-1)} - \frac{34}{25} \frac{\zeta'(-3)}{\zeta(-3)} - \frac{72}{5} \left[ 3 \mathfrak{N}(3, 2z) \right. \\
& \left. \left. + 8 \mathfrak{N}(3, z) - 12 \hat{\mu}^2 \mathfrak{N}(1, 2z) - 2(1 + 8 \hat{\mu}^2) \mathfrak{N}(1, z) + 12i \hat{\mu} \left( \mathfrak{N}(2, z) + \mathfrak{N}(2, 2z) \right) - i \hat{\mu} (1 + 12 \hat{\mu}^2) \mathfrak{N}(0, z) \right] \right] \\
& - \frac{15}{2} \left( 1 + 12 \hat{\mu}^2 \right) \left( 2 \ln \frac{\hat{\Lambda}}{2} - 1 - \mathfrak{N}(z) \right) \hat{m}_D \left. \right] + \frac{c_A \alpha_s}{3\pi} \frac{s_F \alpha_s}{\pi} \left[ \frac{15}{2 \hat{m}_D} \left( 1 + 12 \hat{\mu}^2 \right) + 90 \frac{\hat{m}_q^2}{\hat{m}_D} \right. \\
& - \frac{235}{16} \left\{ \left( 1 + \frac{792}{47} \hat{\mu}^2 + \frac{1584}{47} \hat{\mu}^4 \right) \ln \frac{\hat{\Lambda}}{2} - \frac{24 \gamma_E}{47} \left( 1 + 12 \hat{\mu}^2 \right) + \frac{319}{940} \left( 1 + \frac{2040}{319} \hat{\mu}^2 + \frac{38640}{319} \hat{\mu}^4 \right) - \frac{268}{235} \frac{\zeta'(-3)}{\zeta(-3)} \right. \\
& - \frac{144}{47} \left( 1 + 12 \hat{\mu}^2 \right) \ln \hat{m}_D - \frac{44}{47} \left( 1 + \frac{156}{11} \hat{\mu}^2 \right) \frac{\zeta'(-1)}{\zeta(-1)} - \frac{72}{47} \left[ 4i \hat{\mu} \mathfrak{N}(0, z) + \left( 5 - 92 \hat{\mu}^2 \right) \mathfrak{N}(1, z) + 144i \hat{\mu} \mathfrak{N}(2, z) \right. \\
& \left. \left. + 52 \mathfrak{N}(3, z) \right] \right\} + \frac{315}{4} \left\{ \left( 1 + \frac{132}{7} \hat{\mu}^2 \right) \ln \frac{\hat{\Lambda}}{2} + \frac{11}{7} \left( 1 + 12 \hat{\mu}^2 \right) \gamma_E + \frac{9}{14} \left( 1 + \frac{132}{9} \hat{\mu}^2 \right) + \frac{2}{7} \mathfrak{N}(z) \right\} \hat{m}_D \left. \right] \\
& + \frac{c_A \alpha_s}{3\pi} \left[ - \frac{15}{4} + \frac{45}{2} \hat{m}_D - \frac{135}{2} \hat{m}_D^2 - \frac{495}{4} \left( \ln \frac{\hat{\Lambda}_g}{2} + \frac{5}{22} + \gamma_E \right) \right] + \left( \frac{c_A \alpha_s}{3\pi} \right)^2 \left[ \frac{45}{4 \hat{m}_D} - \frac{165}{8} \left( \ln \frac{\hat{\Lambda}_g}{2} \right. \right. \\
& \left. \left. - \frac{72}{11} \ln \hat{m}_D - \frac{84}{55} - \frac{6}{11} \gamma_E - \frac{74}{11} \frac{\zeta'(-1)}{\zeta(-1)} + \frac{19}{11} \frac{\zeta'(-3)}{\zeta(-3)} \right) + \frac{1485}{4} \left( \ln \frac{\hat{\Lambda}_g}{2} - \frac{79}{44} + \gamma_E - \ln 2 - \frac{\pi^2}{11} \right) \hat{m}_D \right] \left. \right] \left. \right]
\end{aligned}$$

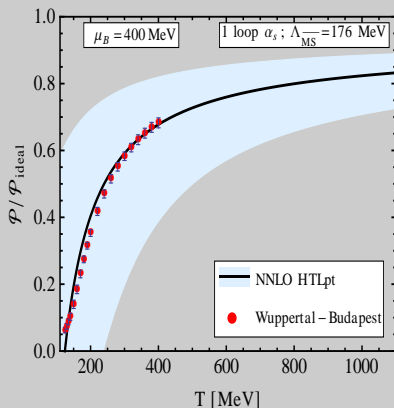
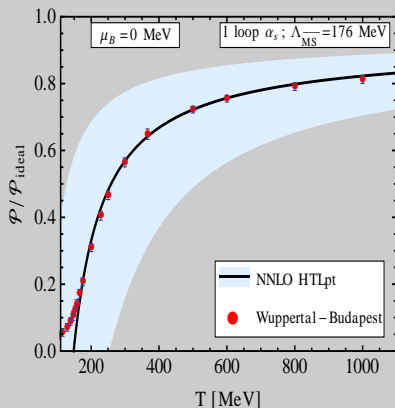
# NNLO pressure for QCD HTL perturbation theory



- Thick Black Line: Renormalization Scale  $\Lambda = 2\pi\sqrt{T^2 + \mu^2}/\pi^2$

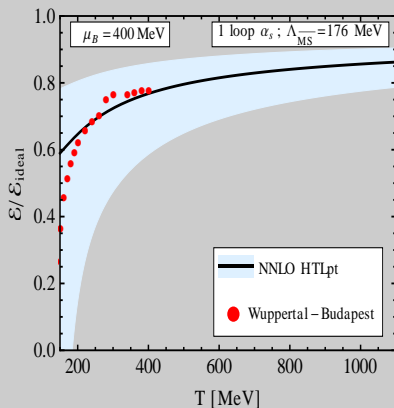
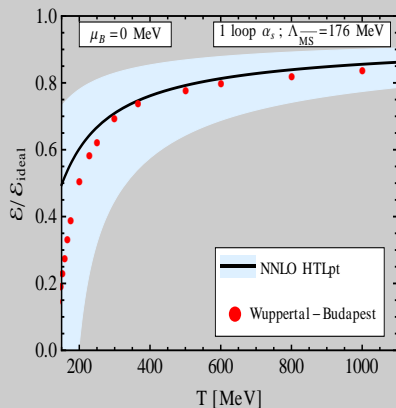


# NNLO pressure for QCD HTL perturbation theory



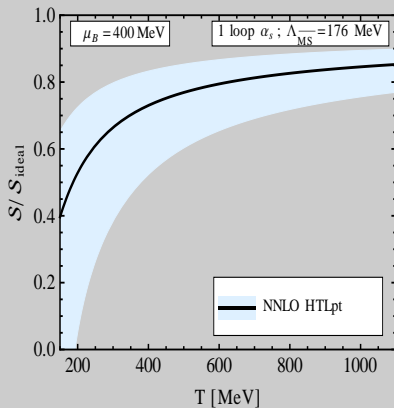
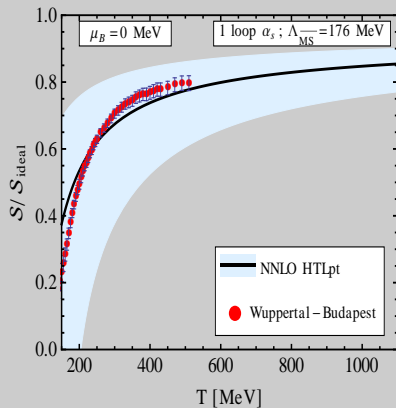
- Thick Black Line: Renormalization Scale  $\Lambda = 2\pi\sqrt{T^2 + \mu^2}/\pi^2$
- Band : Varying center value by factor of 2.

# Energy Density



Lattice data have been extracted using:  $\mathcal{E} = 3\mathcal{P} + I$

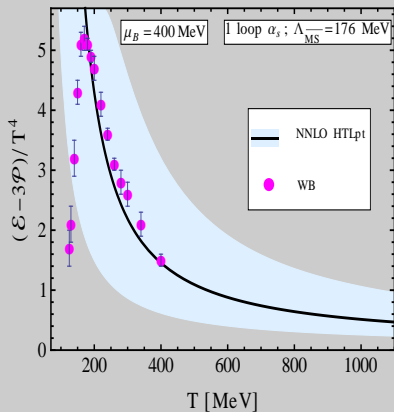
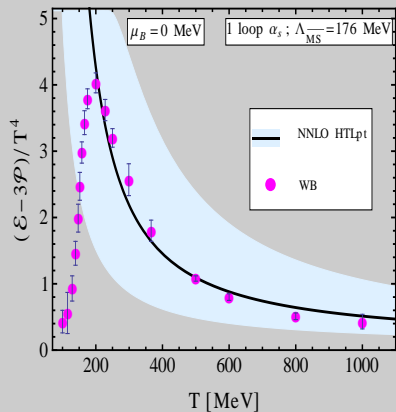
# Entropy Density





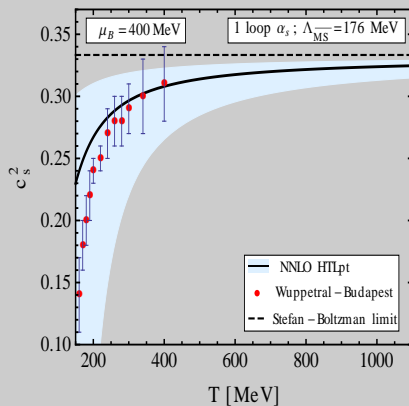
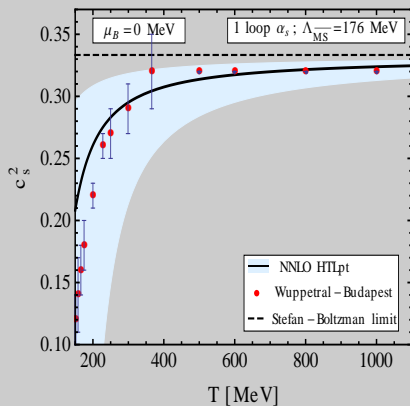
# Trace Anomaly

$$\text{Trace Anomaly} = \mathcal{E} - 3\mathcal{P}$$



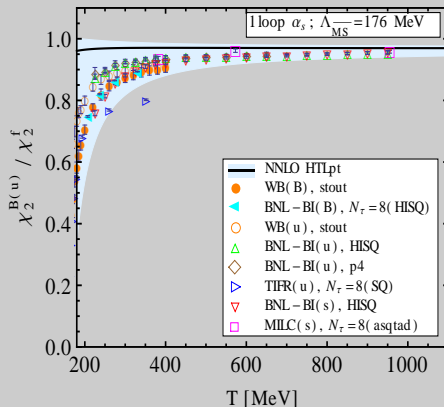
# Speed of Sound

$$c_s^2 = \frac{\partial \mathcal{P}}{\partial \mathcal{E}}$$



# Second order Quark Number Susceptibility

$$\chi_2^u = \left. \frac{\partial^2 \mathcal{P}}{\partial \mu^2} \right|_{\mu \rightarrow 0}$$

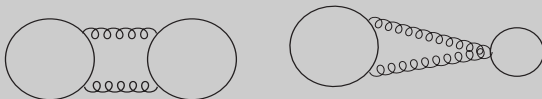


## Fourth order Quark Number Susceptibility

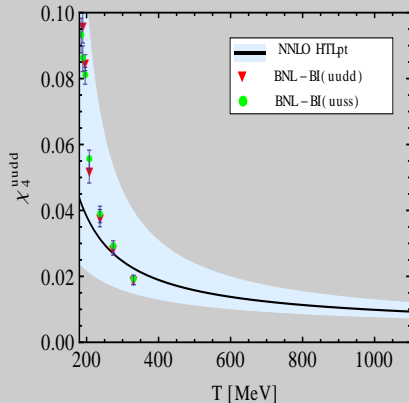
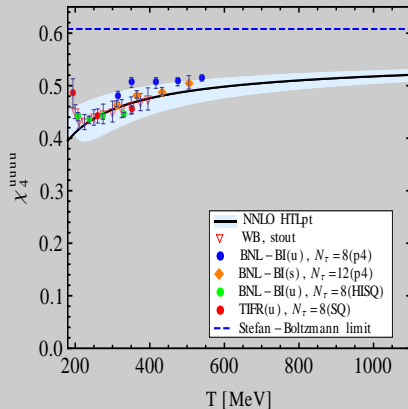
Diagonal Susceptibility  $\chi_4^u = \frac{\partial^4 \mathcal{P}}{\partial \mu^4}$

Off-diagonal Susceptibility  $\chi_4^{uudd} = \frac{\partial^4 \mathcal{P}}{\partial \mu_u^2 \partial \mu_d^2}$ .

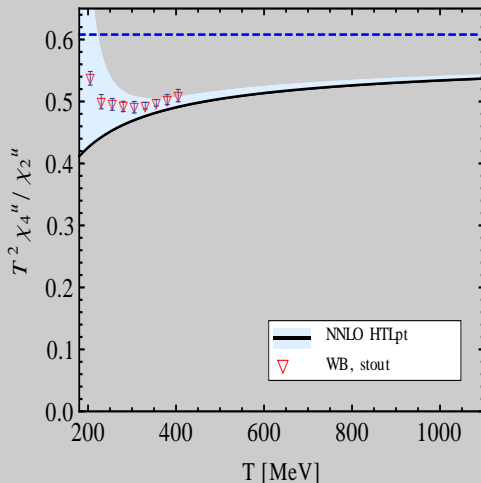
The following two diagrams will contribute to only off-diagonal Susceptibility  $\chi_4^{uudd}$ .



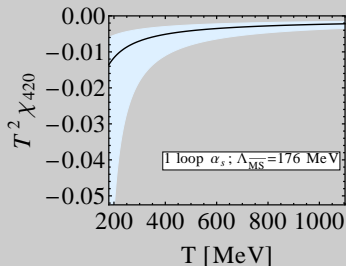
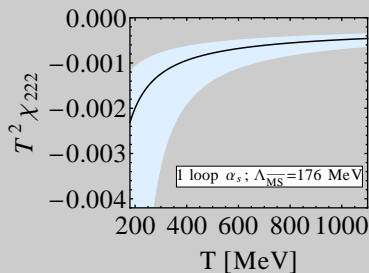
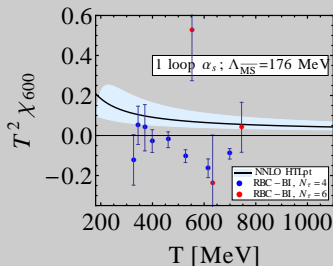
# Fourth order Quark Number Susceptibility



# Fourth/second order Quark Number Susceptibility



# Sixth order Quark Number Susceptibility



# Baryon number susceptibilities

$$\chi_B^n(T) \equiv \left. \frac{\partial^n \mathcal{P}}{\partial \mu_B^n} \right|_{\mu_B=0} .$$

$$\chi_2^B = \frac{1}{9} \left[ \chi_2^{uu} + \chi_2^{dd} + \chi_2^{ss} + 2\chi_2^{ud} + 2\chi_2^{ds} + 2\chi_2^{us} \right] ,$$

and

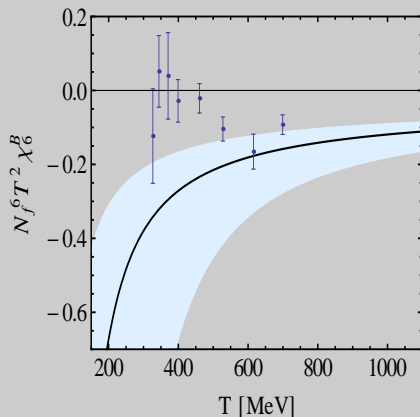
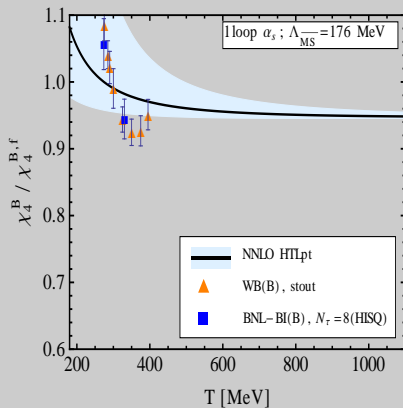
$$\begin{aligned} \chi_4^B = \frac{1}{81} \left[ \chi_4^{uuuu} + \chi_4^{dddd} + \chi_4^{ssss} + 4\chi_4^{uuud} + 4\chi_4^{uuus} \right. \\ + 4\chi_4^{dddu} + 4\chi_4^{ddds} + 4\chi_4^{sss u} + 4\chi_4^{sssd} + 6\chi_4^{uudd} \\ \left. + 6\chi_4^{ddss} + 6\chi_4^{uuss} + 12\chi_4^{uuds} + 12\chi_4^{ddus} + 12\chi_4^{ssud} \right] . \end{aligned}$$

For  $\mu_u = \mu_d = \mu_s = \mu_B/3$ ,

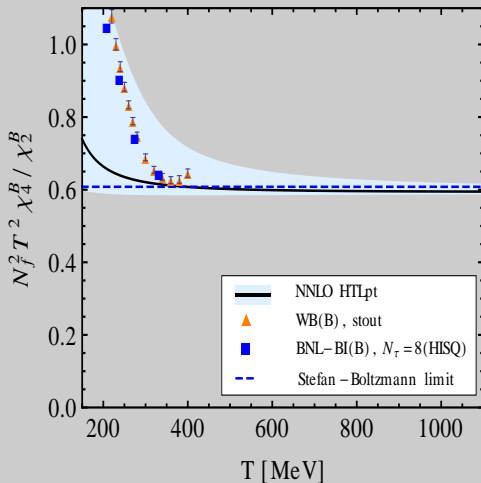
$$\chi_2^B = \frac{1}{3} \chi_2^{uu} \quad \chi_4^B = \frac{1}{27} \left[ \chi_4^{uuuu} + 6\chi_4^{uudd} \right]$$



# Baryon number susceptibilities



# Fourth/second order Baryon Number Susceptibility

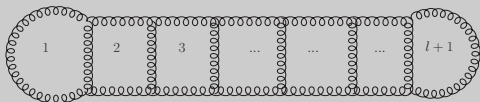


# Conclusions

- I have discussed about thermodynamic quantities in leading as well as beyond leading order using HTLpt.
- Thermodynamical potential produce correct perturbative order upto  $g$ ,  $g^3$  and  $g^5$  if one expands for small  $g$  in case of one loop, two loop and three loop respectively.
- NNLO pressure is completely analytic and does not depend on any free parameter except the choice of the renormalization scale.
- For three loop case, we found good agreement between our results and LQCD results down to temperature  $\sim 250$  MeV.

# Back up Slides

# Linde's Problem



$$\text{Gluon propagator} = \sum_n \frac{1}{\omega_n^2 + k^2 + m^2} \quad \omega_n = 2\pi nT$$

$m$  = some screening mass.

The leading infra-red can be estimated by power counting in partition function as

$$Z_l \sim g^{2l} \left( T \int d^3k \right)^{l+1} k^{2l} (k^2 + m^2)^{-3l}$$

- $l < 3$ :  $Z_l$  is IR regular.
- $l = 3$ :  $Z_l \sim g^6 T^4 \log \left( \frac{T}{m} \right)$
- $l > 3$ :  $Z_l \sim g^6 T^4 \left( \frac{g^2 T}{m} \right)^{l-3}$

# Linde's Problem

- For longitudinal gluons, the screening mass  $m_{el} \sim gT$ . So for  $l > 3$ ,  $Z_l \sim g^{l+3}T^4$ .
- For transverse gluons, the screening mass  $m_{mag} \sim g^2T$ , So for  $l > 3$ ,  $Z_l \sim g^6T^4$ .

Which is a complete failure of Perturbation theory.

# Running coupling

QCD running coupling:

$$\alpha_s(\Lambda) = \frac{g(\Lambda)^2}{4\pi} = \frac{12\pi}{(11N_c - 2N_f) \log\left(\Lambda^2/\Lambda_{\overline{\text{MS}}}^2\right)}, \quad (2)$$

- $\Lambda \rightarrow$  Renormalization scale.
- The middle line corresponds to  $\Lambda = 2\pi\sqrt{T^2 + \mu^2/\pi^2}$ .
- We fix the QCD scale  $\Lambda_{\overline{\text{MS}}}$  by requiring that  $\alpha_s(1.5\text{GeV}) = 0.326$  which is obtained from lattice measurements *A. Bazavov et al., Phys. Rev. D 86 (2012) 114031*.
- $\alpha_s(1.5\text{GeV}) = 0.326 \implies \Lambda_{\overline{\text{MS}}} = 176 \text{ MeV}$  for one loop  $\alpha_s$ .  
 $\Lambda_{\overline{\text{MS}}} = 316 \text{ MeV}$  for three loop  $\alpha_s$ .

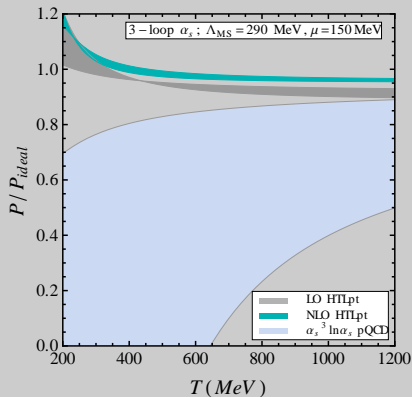
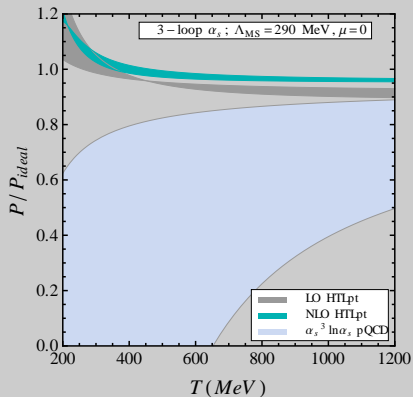
# The value of $\Lambda_{\text{middle}}$

Matsubara frequency:  $\omega_n^b = 2n\pi T$  for boson,  
 $\omega_n^f = (2n + 1)\pi T + i\mu$  for fermion.

At  $\mu = 0$ ,  $\Lambda_{\text{middle}} = \omega_1^b = 2\omega_0^f = 2\pi T$ .

At  $\mu \neq 0$ ,  $\Lambda_{\text{middle}} = 2|\omega_0^f| = 2\pi\sqrt{T^2 + \mu^2/\pi^2}$ .





# Quark Number Susceptibility

JHEP07(2013)184

